



Effect of Hydrogel Molar Composition on the Synthesis of LTA-type Zeolites in the Utilization of Technogenic Silica Gel

Igor N. Pyagay¹ · Yana A. Svakhina¹ · Marina E. Titova¹ · Vladimir V. Miroshnichenko¹ · Victoria R. Dronova¹

Received: 25 March 2024 / Accepted: 2 June 2024 / Published online: 8 June 2024
© The Author(s), under exclusive licence to Springer Nature B.V. 2024

Abstract

Resource saving and creation of environmentally safe environment are the guidelines of modern world policy in the field of waste management. This paper considers a possible method of utilization of a by-product of aluminum fluoride production—silica gel—as an alternative high-silica raw material for hydrothermal synthesis of LTA-type zeolites. To obtain synthetic zeolites, industrial silica gel was subjected to sulfuric acid purification and used to obtain one of the hydrogel components—sodium silicate. As a result of investigation of the influence of hydrogel molar composition on the phase composition of the obtained samples, the optimal molar ratios of $\text{SiO}_2:\text{Al}_2\text{O}_3$, $\text{Na}_2\text{O}:\text{Al}_2\text{O}_3$ and $\text{H}_2\text{O}:\text{SiO}_2$ were identified. The phase composition of the obtained samples and morphological pattern were evaluated using X-ray diffraction and scanning electron microscopy techniques. According to the obtained results, the use of hydrogel of composition $1.8\text{SiO}_2:\text{Al}_2\text{O}_3:4\text{Na}_2\text{O}:28\text{H}_2\text{O}$ allows to obtain a monophase of LTA type zeolite with high ion exchange capacity, the particles of which have a regular cubic shape with the size of the main fraction up to 10 μm .

Keywords Silica gel · Zeolites · Liquid glass · Purification · Hydrothermal synthesis · Ion exchange capacity

1 Introduction

The highest priority in the field of environmental protection is waste management with the aim of their involvement in the production cycle of recycling [1–3]. Despite the benefits of industrial waste storage, the existing sludge ponds occupy large areas, and the waste, in turn, has an unfavorable impact on the environment [4, 5]. Modern trends in waste management involve the utilization of accumulated resources to produce new materials of commercial value [6–8].

Currently, the by-product of aluminum fluoride production is of great interest in the world scientific community as a promising silicon-containing resource due to the content of silicon dioxide in dry matter up to 70% [9, 10]. Industrial production of 1 ton of aluminum fluoride is accompanied by the formation of 0.85 to 2.85 tons of hydrated silica gel, resulting in more than 45 000 tons of waste per month from Russian enterprises alone. At the same time, similar production facilities also operate in the CIS countries and the Baltic States.

The main problem associated with the use of industrial silica gel is the content of fluorine and aluminum impurities greater than 30% in dry matter [11]. Since the formation of aluminum fluoride occurs as a result of the interaction of aluminum hydrate with excess silicofluoric acid, more than 80% of fluorine impurities in man-made silica gel are in the form of fluorides (F^-) and about 20% are silicofluoride ion compounds (SiF_6^{2-}) [12, 13].

In most cases in industrial production of aluminum fluoride, excess silicofluoric acid is used, which leads to the formation of waste with a low pH value and the manifestation of chemisorption properties of silica gel concerning fluoride ions. The high content of impurities in industrial silica gel limits its use in pure form for the production of

✉ Yana A. Svakhina
y_svakhina@mail.ru

Igor N. Pyagay
igor-pya@yandex.ru

Marina E. Titova
marina-titova-2000@mail.ru

Vladimir V. Miroshnichenko
vovamir02@mail.ru

Victoria R. Dronova
vilka.dronova17a@mail.ru

¹ Empress Catherine II Saint Petersburg Mining University, 2, 21st Line, St. Petersburg 199106, Russia

silicate alkaline solutions, because the impurities of silicofluoride ions inhibit this process. Aluminum ions transferred to the solution as a result of alkaline treatment as well as fluoride ions have a greater negative impact on the purity of the finished product. As a result, the problem of purification and modification of industrial silica gel in the scientific and technical literature is of increased interest. Among the most common methods of silica gel purification, special attention is paid to the method of leaching with mineral acids, metal hydroxides, and other inorganic reagents [14–16].

In the absence of impurities, silica gel can be used as an independent product, in the form of amorphous silica powder for the production of reinforced rubber composites [17, 18], high-strength concrete [19, 20] and for obtaining more valuable materials on its basis [21]. An example of obtaining various materials based on amorphous silica is the synthesis of liquid glass by the direct alkaline dissolution of silica gel and subsequent hydrothermal synthesis of zeolites [22–24].

The demand for zeolites on the world market is primarily due to their unique surface properties. The high specific surface area of zeolites is due to the developed and ordered structure of channels and cells, due to which zeolites are widely used in the processes of sorption, catalysis, and ion exchange.

Despite the distribution in nature of such zeolites as clinoptilolite, mordenite, and Chabazite [25, 26] synthetic zeolites of types A, X, Y and NaPl are of particular value for industrial applications. [27–29]. The global synthetic zeolites market is segmented into three major production products: catalyst components, adsorbents and synthetic detergents. The growing demand for inorganic synthesis products is largely attributed to the increasing share of global production of detergents and adsorbents based on synthetic zeolites and sodium silicate [30, 31].

The main zeolite-containing component of detergents is a zeolite of structural type LTA, characterized by high ion-exchange capacity concerning Ca^{2+} , Mg^{2+} , and various heavy metal cations [32, 33]. The ability of LTA-type zeolite to ion exchange calcium and magnesium cations is the basis for their application as components of detergents that reduce water hardness and for water treatment processes. In addition, zeolite-containing detergents are a more environmentally friendly alternative to phosphate detergents, since wastewater containing phosphate ions contributes to the eutrophication of water bodies and harmful algal blooms [34, 35]. To resolve this problem, some countries, including EU countries and the USA, have banned the use of phosphate-based detergents, increasing in demand for zeolite-containing products. With an average annual growth rate of zeolite and sodium silicate production of 4 and 2.5% [36, 37], respectively, the main task for the scientific community is to find alternative raw materials to increase production capacity.

Thus, the demand for zeolites in the world market can be increased by using silica gel as a promising silicon-containing source for the production of one of the hydrogel components—sodium silicate, which is also an independent commodity product.

In this paper, the authors present data concerning the use of purified silica gel, obtained as a result of sulfuric acid purification, in the process of obtaining liquid glass for hydrothermal synthesis of zeolites of structural type LTA. In addition, the paper presents studies of the influence of the molar composition of hydrogel obtained based on liquid glass from silica gel on the phase composition of synthetic zeolite of LTA type.

2 Materials and Methods

2.1 Materials

The object of the study—industrial silica gel, chemical composition 59.3 wt.% SiO_2 , 13.3 wt.% Al, 16.6 wt.% F with moisture content more than 50%, was obtained from the Russian enterprise for the production of aluminum fluoride. The silica gel was an amorphous silica powder with a particle size of the main fraction from 25 to 100. Aluminum hydroxide and caustic soda, used for the preparation of hydrogel components, as well as other reagents had a purity of more than 98 wt.% and were obtained from commercial sources.

2.2 Preparation of Silica Gel

Purification of industrial silica gel was carried out by treatment with a solution of sulfuric acid with a concentration of 1.0 wt.% of feedstock at a temperature of 95 °C and constant stirring in a closed reactor. Upon completion of the purification process, the resulting suspension was filtered, and the solid phase, which is amorphous silica, was washed with distilled water to a pH value of washing water 7–8 and dried at a temperature above 100 °C for at least 3 h.

2.3 Preparation of Precursors

Purified silica gel was used to obtain silica-containing components of hydrogel-liquid glass. Sodium silicate was obtained by batch dissolution of the obtained silicon dioxide in a solution of sodium hydroxide with a concentration of 12.5 wt.% at a temperature of 100 °C and intensive stirring for 4.5 h [38]. The aluminum-containing hydrogel component, sodium aluminate, was obtained by dissolving aluminum hydroxide in aqueous sodium hydroxide solution at 95 °C for 5 h with constant stirring.

The masses of components for the processes were calculated taking into account the content of Na₂O 300–320 g/l and Al₂O₃ 270–290 g/l in sodium aluminate solution and Na₂O 80–90 g/l and SiO₂ 240–270 g/l in liquid glass. The prepared solutions were filtered under a vacuum to remove suspended particles that could act as additional crystallization centers during zeolite synthesis. In the case of aluminate solution, the removal of suspended particles also prevents its degradation and prevents re-precipitation of aluminum hydroxide precipitation.

2.4 Hydrothermal Synthesis of LTA-type Zeolites

For the hydrothermal synthesis of zeolites, two hydrogel components, preheated to 50 °C, were mixed in amounts providing hydrogel molar ratios of 1.3 to 2.0 SiO₂:Al₂O₃, 3 to 5 Na₂O:Al₂O₃, and 30 to 100 H₂O:SiO₂, and incubated for 10 min under vigorous stirring to obtain a homogeneous mixture. The resulting hydrogel was placed in a closed reactor, heated to 95 °C, and incubated for 60 min at 100 rpm stirring for hydrothermal reaction [39]. At the end of the crystallization process, the aluminosilicate solid phase was separated by filtration and washed with heated distilled water until the wash water was neutral. The separated precipitate was first dried at room temperature for 24 h, then at 105 °C until the moisture was removed.

2.5 Me²⁺ Exchange of Zeolite LTA

The cation exchange capacity (CEC) of the obtained LTA-type zeolite was determined by its ability to exchange Ca²⁺ ions in calcium chloride solution with a concentration of 1 g/l. A suspension of zeolite was placed in the solution under study at the liquid-to-solid ratio = 1/500 and incubated under isothermal conditions at temperatures of 25 °C for 60 min in a GFL-3032 shaker-incubator at a shaking frequency of 100 rpm. The CEC value (mEq/100g) concerning Ca²⁺ ions was determined as the difference of concentrations at the beginning and the end of the ion exchange process according to formula 1.

$$CEC(Me^{2+}) = \frac{C_0 - C}{f_{eq} \cdot m} \cdot 100 \quad (1)$$

where C_0 and C are the concentration of Ca²⁺ ions at the beginning and end of the process, g/l; f_{eq} is the equivalence factor; m is the mass of the zeolite suspension, g.

2.6 Characterization and Analysis

The elemental composition of the initial industrial silica gel was carried out by atomic emission spectroscopy with inductively coupled plasma (ICP-AES) on an ICPE-9000

Shimadzu spectrometer and by X-ray fluorescence method on an XRF-1800 Shimadzu wave dispersive X-ray fluorescence spectrometer.

Fourier-transform infrared spectroscopic (FTIR) analysis of silica gel before and after the purification process was performed on a Shimadzu IRAffinity-1 instrument in the wave number range of 400–4000 cm⁻¹ with a resolution of 2 cm⁻¹ for 40 scans.

The content of silicon compounds in terms of silicon dioxide in the obtained solutions was analyzed on a Shimadzu EDX 7000P X-ray fluorescence instrument using calibration curves, for the construction of which the state standard sample of silicon ions was used.

Identification of phases for the obtained zeolite samples was carried out by powder X-ray diffraction (XRD) on a Shimadzu XRD-7000 device with CuK α -radiation, operating at a current of 30 mA and a shortening voltage of 40 kV. X-ray radiographs were taken over a range of diffraction angles (2θ) from 5 to 50° with a scanning speed of 1 deg/min. The presence of aluminium fluoride phase was determined by principal interplanar distances $d_{hkl} = 5.46, 3.86, 3.65, 3.30, 3.03, 2.73, 2.65, 2.51, 2.44, 2.18, 2.1, 2.03$ and 1.93 Å. The presence of an LTA-type zeolite phase was determined by the principal d -distances $d_{hkl} = 12.305, 8.701, 7.104, 4.102, 3.710, 3.289, 2.984$ and 2.623 Å.

The morphological pattern of the obtained samples was studied on a TescanVega3 instrument by scanning electron microscopy (SEM). The image was obtained from secondary electrons (SE) in RESOLUTION scanning mode at an accelerating voltage of 20.0 kV.

The particle size distribution was determined using a Microsizer 201C laser particle size analyzer. Before analysis, ultrasonic dispersion of the solution was additionally performed to break agglomerates and prevent particle settling.

3 Results and discussion

3.1 Sulfuric Acid Purification of Silica Gel

As noted earlier, the use of industrial silica gel in its original form to produce sodium silicate solution is limited by the presence of impurities of fluorine and aluminum compounds. According to the data of X-ray diffraction phase analysis of industrial silica gel, presented in Fig. 1a, the character of the XRD patterns indicates the amorphous state of silica gel, in addition, the peaks of the industrial sample indicate the presence of impurities of aluminum and fluorine in the form of AlF₃.

FTIR of the initial silica gel, presented in Fig. 2, confirms the data of X-ray phase analysis, where the absorption in the range of 800 cm⁻¹ indicates the presence of a group [SiO₄]⁴⁻ in the silica gel structure. The vibrational

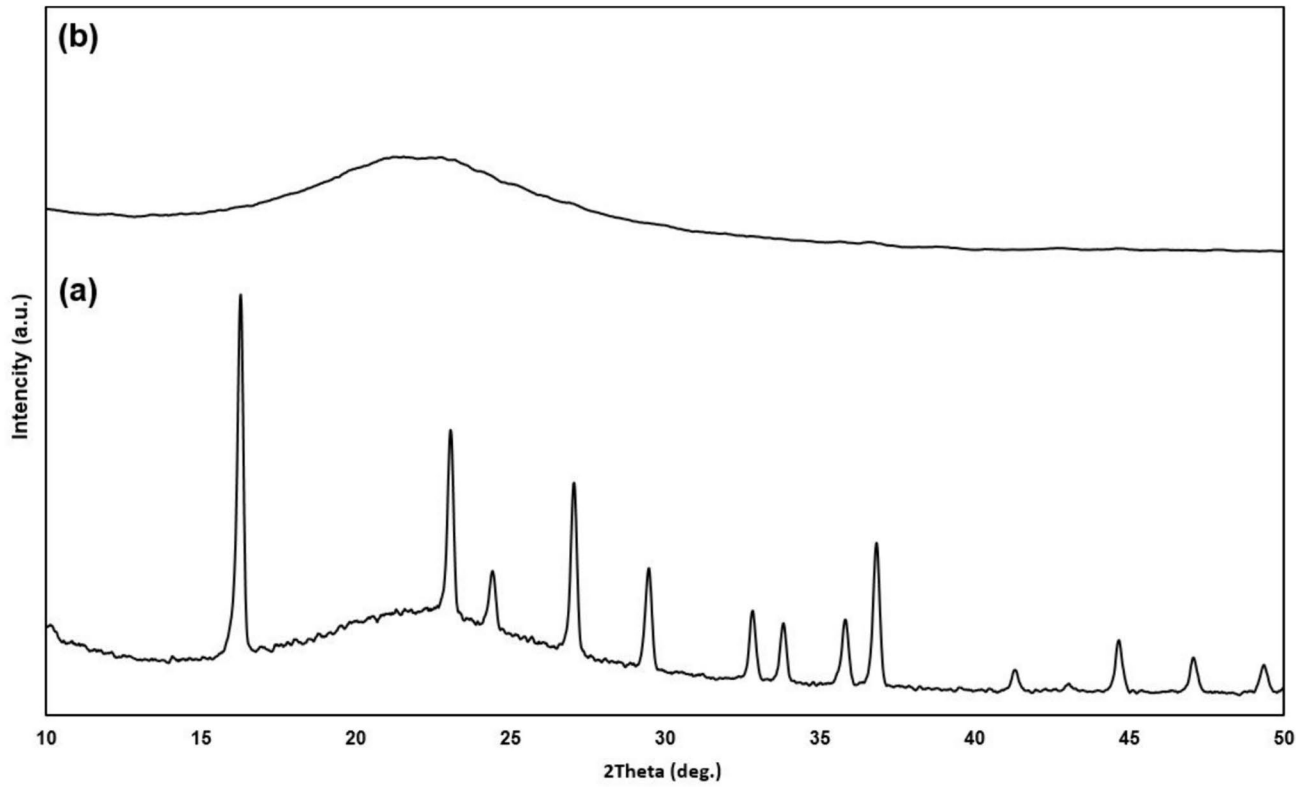


Fig. 1 XRD patterns of silica gel: **a** initial sample; **b** after the purification process

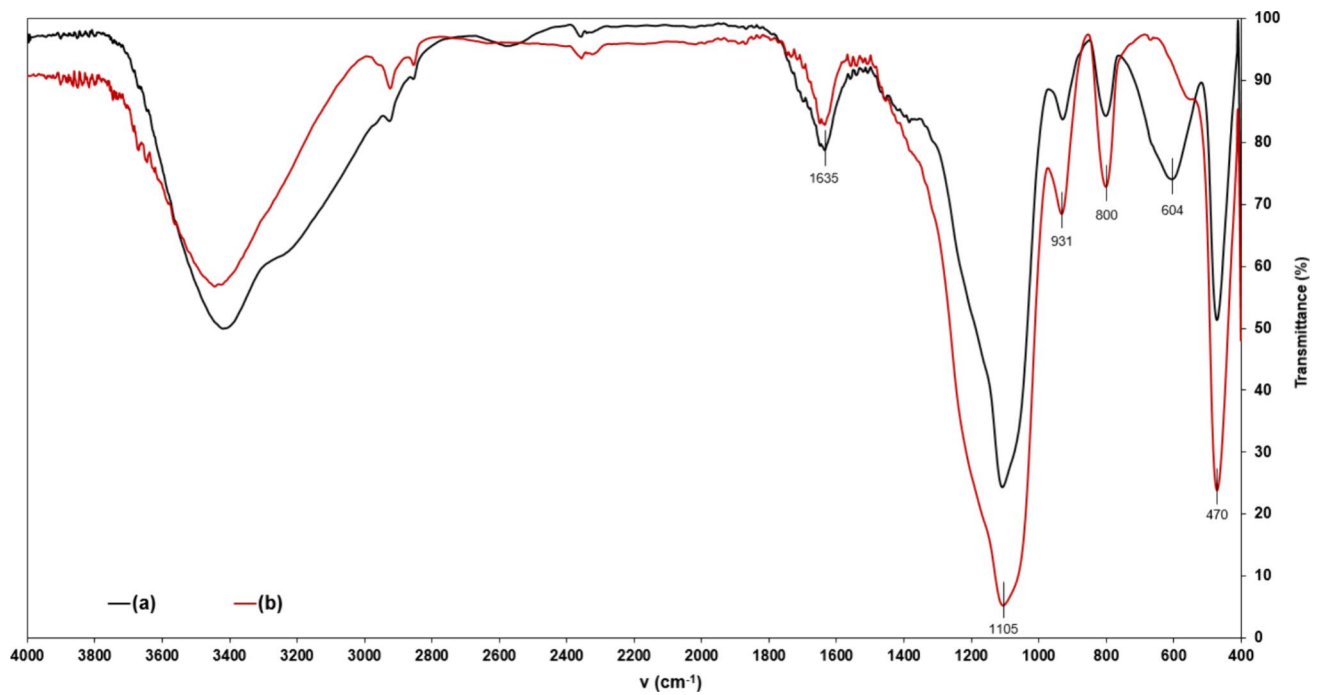


Fig. 2 FTIR spectra of silica gel: **a** of the initial sample; **b** after the purification process

frequencies in the absorption region $1000\text{--}1250\text{ cm}^{-1}$ confirm the presence of Si–O bond in the silica gel structure [40]. The disordered amorphous structure of silicon oxide probably causes a shift in the vibrational frequencies of aluminum fluoride, which were observed in the $550\text{--}750\text{ cm}^{-1}$ region when compared with pure aluminum fluoride [41]. Absorption in the 800 and 930 cm^{-1} region on the FTIR spectra also indicates the possible presence of adsorbed SiF_4 molecules in the silica structure [42].

Purification of industrial silica gel with mineral acids is the most effective way to remove impurities, because silica, which is the target product of purification, does not interact with them, unlike the aluminum and fluorine salts present. At the same time, the treatment of the initial silica gel with alkaline reagents, on the contrary, contributes to a decrease in the proportion of silica in the finished product as a result of its partial leaching in the form of sodium silicate. Thus, for the purification process of silica gel as a reagent, a sulfuric acid concentration of 1 wt.% was.

According to ICP-AES data, as a result of treating industrial silica gel with a slightly concentrated sulfuric acid solution, aluminum impurities were almost completely removed from the silica gel, and the fluoride content decreased to 3.27 wt.%. The FTIR spectra of the purified silica gel presented in Fig. 2b confirm the efficiency of aluminum fluoride removal by sulfuric acid purification due to the absence of absorption in the interval $550\text{--}750\text{ cm}^{-1}$. In addition, the data obtained are confirmed by the absence of characteristic peaks of AlF_3 in the X-ray diffraction pattern of the purified sample presented in Fig. 1b. Fluorine impurities in the purified silica gel are mainly represented in the form of SiF_4 , which is confirmed by the presence of vibrational frequencies in the region of 800 cm^{-1} on the FTIR spectra, but their concentration is markedly reduced.

As a result of the process of sulfuric acid purification of industrial silica gel, an amorphous powder with a silica content of more than 91 wt.% was obtained. Since sodium silicate solution can be used as a source of silicon for hydrothermal synthesis of zeolites, based on the requirements for the quality of silicon-containing raw materials, the SiO_2 content of more than 90 wt.% in the purified silica gel allows use it for the production of liquid glass.

In [38] authors confirmed the possibility of using waste silica gel after sulfuric acid purification to obtain liquid glass with concentrations of Na_2O 80–90 g/l and SiO_2 240–270 g/l with silicate modulus from 2.9 to 3.2. The silicate modulus of the obtained liquid glass is acceptable for the use of this silicate solution to obtain a silica-containing hydrogel component for the synthesis of LTA-type zeolites. The liquid glass obtained with given concentrations was used to carry out a study of the influence of the molar composition of the hydrogel on the phase composition of the obtained zeolites.

3.2 Hydrothermal Synthesis of LTA-type Zeolites

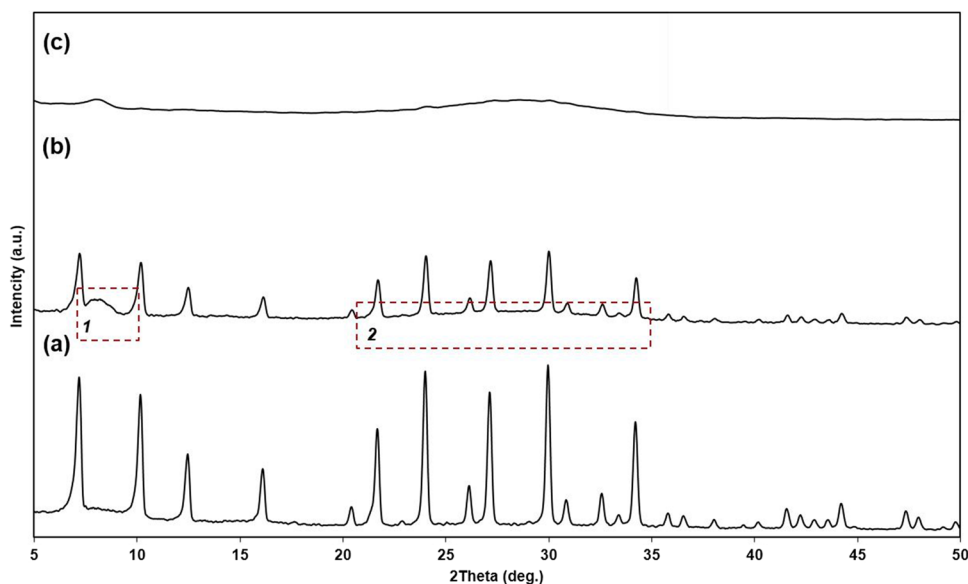
Traditionally, zeolites are obtained by crystallization of hydrogel obtained from pure solutions of sodium silicate and aluminate, aluminum salts, colloidal silica, and other reagents. To conduct further studies on the influence of hydrogel molar composition on the phase composition of zeolites, the authors obtained aluminate and silicate solutions for the hydrothermal synthesis of zeolites of structural type LTA [43, 44]. Despite the availability of information on the molar composition of zeolites of different types, for each type of raw material, these values will differ due to the influence of different process parameters, as well as the mutual influence of the components of the initial mixture [45–47]. Thus, this study is aimed at identifying the optimal composition of the initial hydrogel, the silicon-containing component of which is obtained from the processing of aluminum fluoride production waste.

In this work, the influence of the molar composition of the hydrogel was determined by identifying the optimal ranges of molar ratios of $\text{SiO}_2\text{:Al}_2\text{O}_3$, $\text{Na}_2\text{O:Al}_2\text{O}_3$, and $\text{H}_2\text{O:SiO}_2$, at which the formation of LTA-type zeolite monophase would be observed in the obtained sample.

First of all, the influence of the silicon modulus value was determined, since this parameter has a direct influence on the type and structure of the obtained zeolite. The influence was evaluated by changing the molar ratio of $\text{SiO}_2\text{:Al}_2\text{O}_3$ in the range from 1.3 to 2.4, while the ratios of $\text{Na}_2\text{O:Al}_2\text{O}_3$ and $\text{H}_2\text{O:SiO}_2$ remained unchanged throughout the experiment and were equal to 4 and 50, respectively. According to the results of the XRD analysis presented in Fig. 3, changing the molar ratio of $\text{SiO}_2\text{:Al}_2\text{O}_3$ from 1.5 to 1.8 resulted in the monophase of LTA-type zeolite. A comparison of peak intensity values on X-ray diffraction patterns of the obtained samples showed that at $\text{SiO}_2\text{:Al}_2\text{O}_3 = 1.8$ the zeolite particles had the highest crystallinity. At ratio $\text{SiO}_2\text{:Al}_2\text{O}_3$ less than 1.5 and more than 1.8 in addition to the phase of zeolite LTA also was present a phase of amorphous aluminosilicate, which was identified by X-ray diffraction at sites 1 and 2. At a larger deviation of the $\text{SiO}_2\text{:Al}_2\text{O}_3$ ratio from the optimum range, an increase in the proportion of the amorphous aluminosilicate phase was observed. Further increase of $\text{SiO}_2\text{:Al}_2\text{O}_3$ ratio up to 2.4 led to the fact that the crystalline phase of LTA type zeolite was practically absent, and the investigated sample was represented mainly by the amorphous phase of aluminosilicate.

The effect of alkalinity was determined by varying the $\text{Na}_2\text{O:Al}_2\text{O}_3$ ratio between 3 and 5 at other ratios $\text{SiO}_2\text{:Al}_2\text{O}_3 = 1.8$ and $\text{H}_2\text{O:SiO}_2 = 50$. In the sample obtained at $\text{Na}_2\text{O:Al}_2\text{O}_3$ ratios less than 3, the formation of a mixture of crystalline and amorphous phases was observed. The presence of the amorphous aluminosilicate phase is probably due to the low content of Na^+ and OH^- ions involved in the

Fig. 3 X-ray diffraction patterns of the obtained samples: **a** $\text{SiO}_2:\text{Al}_2\text{O}_3=1.8$; $\text{Na}_2\text{O}:\text{Al}_2\text{O}_3=4$; $\text{H}_2\text{O}:\text{SiO}_2=50$; **b** $\text{SiO}_2:\text{Al}_2\text{O}_3=2.0$; $\text{Na}_2\text{O}:\text{Al}_2\text{O}_3=4$; $\text{H}_2\text{O}:\text{SiO}_2=50$; **c** $\text{SiO}_2:\text{Al}_2\text{O}_3=2.4$; $\text{Na}_2\text{O}:\text{Al}_2\text{O}_3=4$; $\text{H}_2\text{O}:\text{SiO}_2=50$



formation of the zeolite lattice [48]. $\text{Na}_2\text{O}:\text{Al}_2\text{O}_3$ ratio from 4 to 5 led to the formation of a crystalline phase of LTA-type zeolite without amorphous inclusions. Further increase of alkalinity did not have a favorable effect on obtaining the crystalline phase of zeolite, since carrying out the process over OH^- ions promotes the transition of LTA-type zeolite to a more stable sodalite phase [48].

To evaluate the effect of dilution of the initial hydrogel, the $\text{H}_2\text{O}:\text{SiO}_2$ ratio was varied from 30 to 100 with constant $\text{SiO}_2:\text{Al}_2\text{O}_3=1.8$ and $\text{Na}_2\text{O}:\text{Al}_2\text{O}_3=4$. The ratio $\text{H}_2\text{O}:\text{SiO}_2$ shows the influence of the dilution degree of the initial hydrogel on the phase composition of the obtained zeolites. As the amount of water in the reaction mixture increases, the nucleation and crystallization stages proceed less intensively, which leads to an increase in the process time [49, 50]. Along with this, when the amount of water decreases, the processes of hydrogel production and crystallization of the mixture become more complicated due to the high viscosity of the initial solutions and the obtained hydrogel.

According to the obtained XRD and SEM images are shown in Figs. 4 and 5, respectively, the ratio $\text{H}_2\text{O}:\text{SiO}_2=50$ is optimal for obtaining LTA-type zeolite monophase. Samples obtained at the range of $\text{H}_2\text{O}:\text{SiO}_2$ ratios from 60 to 80 contained an amorphous aluminosilicate phase, and with an increasing amount of water the share of the zeolite phase decreased significantly. Further increase of this ratio up to 100 resulted in completely amorphous samples without crystalline phase. At $\text{H}_2\text{O}:\text{SiO}_2$ equal to 30 and 40 the obtained samples were represented mainly by the LTA zeolite phase, but during the experiment difficulties in mixing the initial solutions were noted due to the high viscosity of the hydrogel.

The study of the morphology of LTA zeolite obtained from hydrogel of molar composition

$1.8\text{SiO}_2:\text{Al}_2\text{O}_3:4\text{Na}_2\text{O}:50\text{H}_2\text{O}$ showed that zeolite particles have regular cubic shapes with well-defined faces. The size of most of the particles, according to SEM images, did not exceed $10\ \mu\text{m}$, which is also confirmed by the data of particle size analysis. According to the particle size distribution of the obtained sample, particles with diameters up to $10\ \mu\text{m}$ make up more than 95%. The remaining particles are between 10 and $20\ \mu\text{m}$ in size, and no particles larger than $20\ \mu\text{m}$ were found. The particle size less than $10\ \mu\text{m}$ satisfies the requirements for the application of the obtained LTA-type zeolite as an additive to detergents [51]. As a result of the study of the ion exchange capacity of zeolite about Ca^{2+} ions the CEC value for the obtained sample at $25\ ^\circ\text{C}$ was $550\ \text{mEq}/100\ \text{g}$, which is a high indicator of the required cation exchange capacity of $450\ \text{mEq}/100\ \text{g}$ to reduce water hardness in water treatment processes [52].

Thus, the molar ratios $\text{SiO}_2:\text{Al}_2\text{O}_3=1.8$, $\text{Na}_2\text{O}:\text{Al}_2\text{O}_3=4$, and $\text{H}_2\text{O}:\text{SiO}_2=50$ of the initial hydrogel obtained using silica gel-based liquid glass are the most optimal for hydrothermal synthesis of LTA structural type zeolites with high ion exchange capacity.

4 Conclusions

This work is devoted to the issue of utilization of a by-product of aluminum fluoride production—silica gel—to obtain demanded silicon-containing materials. According to the results of the study of the composition of industrial silica gel, it was found that fluorine and aluminum impurities, contained in the amount of 13.3 wt.% Al, 16.6 wt.% F, are present in the initial sample in the form of compounds AlF_3 and SiF_4 . According to the data of atomic emission spectroscopy, after sulfuric acid purification of silica gel,

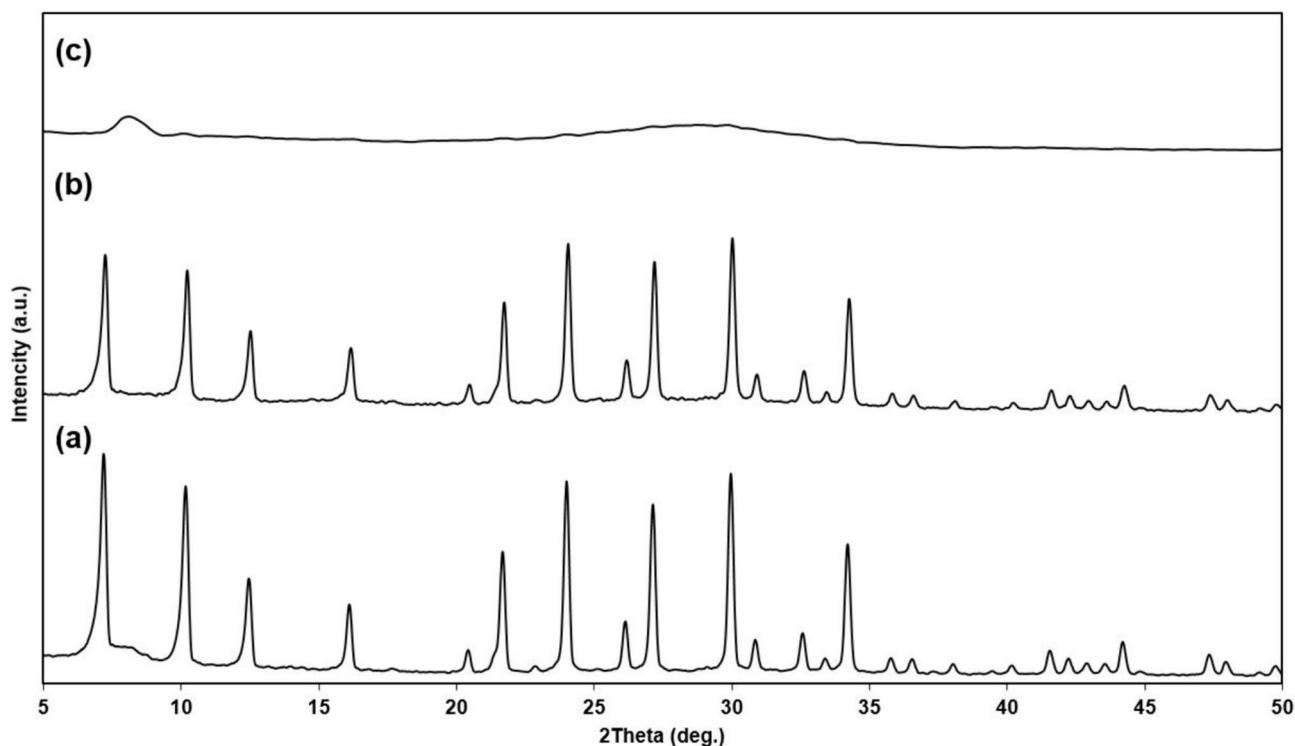


Fig. 4 X-ray diffraction patterns of the obtained samples: **a** $\text{SiO}_2:\text{Al}_2\text{O}_3=1.8$; $\text{Na}_2\text{O}:\text{Al}_2\text{O}_3=4$; $\text{H}_2\text{O}:\text{SiO}_2=40$; **b** $\text{SiO}_2:\text{Al}_2\text{O}_3=1.8$; $\text{Na}_2\text{O}:\text{Al}_2\text{O}_3=4$; $\text{H}_2\text{O}:\text{SiO}_2=60$; **c** $\text{SiO}_2:\text{Al}_2\text{O}_3=1.8$; $\text{Na}_2\text{O}:\text{Al}_2\text{O}_3=4$; $\text{H}_2\text{O}:\text{SiO}_2=90$

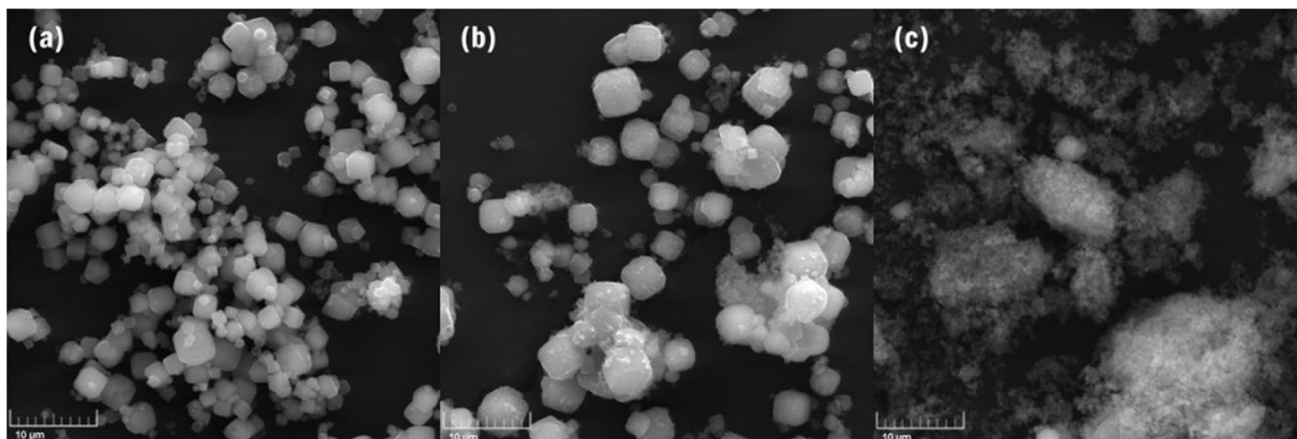


Fig. 5 SEM images of the obtained samples: **a** $\text{SiO}_2:\text{Al}_2\text{O}_3=1.8$; $\text{Na}_2\text{O}:\text{Al}_2\text{O}_3=4$; $\text{H}_2\text{O}:\text{SiO}_2=40$; **b** $\text{SiO}_2:\text{Al}_2\text{O}_3=1.8$; $\text{Na}_2\text{O}:\text{Al}_2\text{O}_3=4$; $\text{H}_2\text{O}:\text{SiO}_2=60$; **c** $\text{SiO}_2:\text{Al}_2\text{O}_3=1.8$; $\text{Na}_2\text{O}:\text{Al}_2\text{O}_3=4$; $\text{H}_2\text{O}:\text{SiO}_2=90$

aluminum impurities were removed almost completely, and the fluorine content decreased significantly. The possibility of using purified silica gel, which has an amorphous structure, to produce liquid glass as a silicon-containing hydrogel component in the hydrothermal synthesis of zeolites was shown.

The dependence of the phase composition and crystallinity of the obtained zeolites on the influence of the molar composition of the hydrogel obtained by mixing aluminum- and silicon-containing components was determined. According to the results of the study, the optimal molar ratios of the initial hydrogel were determined, at which the formation

of LTA-type zeolite monophase with a high degree of crystallinity and the value of cation-exchange capacity for Ca^{2+} ions 550 mEq/100 g was observed. More than 95% of zeolite particles obtained from hydrogel with composition $\text{SiO}_2:\text{Al}_2\text{O}_3 = 1.8$, $\text{Na}_2\text{O}:\text{Al}_2\text{O}_3 = 4$, and $\text{H}_2\text{O}:\text{SiO}_2 = 50$, had a size up to 10 μm , and during the study of the morphology of this sample, it was determined that all particles are represented by crystals of cubic shape, characteristic of LTA type zeolite.

Acknowledgements The investigation was conducted at the Scientific Center “Issues of Mineral and Technogenic Resources Processing” with the involvement of the laboratory base of the Center for Collective Use of Empress Catherine II Saint Petersburg Mining University.

Author Contributions All authors contributed to the conception and design of the study. Material preparation, data collection and formal analysis were carried out by M.E., V.V. and V.R.. Data curation and validation was done by I.N., Ya.A. and M.E. Ya.A. and M.E. wrote the main text of the manuscript, I.N. edited and reviewed the manuscript. All authors read and approved the final manuscript.

Funding The authors state that they received no financial support for the research and preparation of this manuscript.

Data Availability No datasets were generated or analysed during the current study.

Declarations

Ethics Approval The authors confirm that this manuscript is original, has not been previously published in whole or in part, and is not currently under consideration for publication in another journal.

Consent to Participate and Publication The authors consent to participation and publication of the manuscript.

Competing Interests The authors declare no competing interests.

References

1. Popov G, Bolobov V, Zhuikov I, Zlotin V (2023) Development of the kinetic equation of the groove corrosion process for predicting the residual life of oil-field pipelines. *Energies* 16:7067. <https://doi.org/10.3390/en16207067>
2. Bolobov VI, Latipov IU, Zhukov VS, Popov GG (2023) Using the magnetic anisotropy method to determine hydrogenated sections of a steel pipeline. *Energies* 16:5585. <https://doi.org/10.3390/en16155585>
3. Safiullin RN, Safiullin RR, Sorokin KV et al (2024) Integral assessment of influence mechanism of heavy particle generator on hydrocarbon composition of vehicles motor fuel. *Int J Eng* 37:1700–1706. <https://doi.org/10.5829/IJE.2024.37.08B.20>
4. Zubkova O, Alexeev A, Polyanskiy A et al (2021) Complex processing of saponite waste from a diamond-mining enterprise. *Appl Sci* 11:6615. <https://doi.org/10.3390/app11146615>
5. Cheremisina O, Litvinova T, Sergeev V et al (2021) Application of the organic waste-based sorbent for the purification of aqueous solutions. *Water* 13:3101. <https://doi.org/10.3390/w13213101>
6. Gerasimov A, Ustinov I, Zyryanova O (2023) Use of clay-containing waste as pozzolanic additives. *J Min Inst* 260:313–320. <https://doi.org/10.31897/PMI.2023.33>
7. Ponomareva MA, Cheremisina OV, Mashukova YA, Lukyantseva ES (2021) Increasing the efficiency of rare earth metal recovery from technological solutions during processing of apatite raw materials. *J Min Inst* 252:1–10. <https://doi.org/10.31897/PMI.2021.6.13>
8. Litvinova TE, Tsareva AA, Poltoratckaya ME, Rudko VA (2024) The mechanism and thermodynamics of ethyl alcohol sorption process on activated petroleum coke. *J Min Inst*. <https://doi.org/10.21203/rs.3.rs-3308920/v1>
9. Vaiciukynienė D, Jakevicius L, Kantautas A et al (2021) Conversion of silica by-product into zeolites by thermo-sonochemical treatment. *Ultrason Sonochem* 72. <https://doi.org/10.1016/j.ultsonch.2020.105426>
10. Gorlanov ES, Leontev LI (2024) Directions in the technological development of aluminium pots. *J Min Inst* 266:246–259
11. Rudelis V, Dambrauskas T, Grineviciene A, Baltakys K (2019) The prospective approach for the reduction of fluoride ions mobility in industrial waste by creating products of commercial value. *Sustainability* 11:634. <https://doi.org/10.3390/su11030634>
12. Gineika A, Dambrauskas T, Baltakys K (2021) Synthesis and characterisation of wollastonite with aluminium and fluoride ions. *Ceram Int* 47:22900–22910. <https://doi.org/10.1016/j.ceramint.2021.05.003>
13. Gineika A, Baltakys K, Dambrauskas T (2019) The application of silica gel waste for the two-step synthesis of wollastonite in temperature range of 200–950 °C. *J Therm Anal Calorim* 138:2263–2273. <https://doi.org/10.1007/s10973-019-08481-5>
14. Dambrauskas T, Baltakys K, Grineviciene A, Rudelis V (2021) The effect of various hydroxide and salt additives on the reduction of fluoride ion mobility in industrial waste. *Sustainability* 13:1554. <https://doi.org/10.3390/su13031554>
15. Mamchenkov Prokof'ev EAVY (2019) Sodium silicate manufacturing from modified silica gel as by-product of aluminum fluoride. *ChemChemTech* 62:89–93. <https://doi.org/10.6060/ivkk.20196203.5949>
16. Wong EY, Stenstrom MK (2021) The usage of calcium phosphate systems for onsite defluoridation treatment. *J Environ Sci Heal Part A* 56:1189–1195. <https://doi.org/10.1080/10934529.2021.1973311>
17. Kakasor Ismael Jaf D, Ismael Abdulrahman P, Salih Mohammed A et al (2023) Machine learning techniques and multi-scale models to evaluate the impact of silicon dioxide (SiO_2) and calcium oxide (CaO) in fly ash on the compressive strength of green concrete. *Constr Build Mater* 400:132604. <https://doi.org/10.1016/j.conbuildmat.2023.132604>
18. Kornev YV, Semenov NA, Vlasov AN, Valiev KK (2021) Reinforcing effects in elastomeric composites, filled with particles of mineral fillers, based on silicon dioxide and carbon. *J Phys Conf Ser* 1942:012031. <https://doi.org/10.1088/1742-6596/1942/1/012031>
19. Endzhievskaya IG, Demina AV, Lavorenko AA (2020) Synthesis of a mineralizing agent for Portland cement from aluminum production waste. *IOP Conf Ser Mater Sci Eng* 945:012062. <https://doi.org/10.1088/1757-899X/945/1/012062>
20. Kakasor Ismael Jaf D, Abdulrahman AS, Abdulrahman PI et al (2023) Effitoned soft computing models to evaluate the impact of silicon dioxide (SiO_2) to calcium oxide (CaO) ratio in fly ash on the compressive strength of concrete. *J Build Eng* 74:106820. <https://doi.org/10.1016/j.jobe.2023.106820>
21. de Aquino TF, Estevam ST, Viola VO et al (2020) CO_2 adsorption capacity of zeolites synthesized from coal fly ashes. *Fuel* 276:118143. <https://doi.org/10.1016/j.fuel.2020.118143>

22. Tran NM, Nam Y, Yoo H (2022) Fabrication of dendritic fibrous silica nanolayer on optimized water-glass-based synthetic nanosilica from rice husk ash. *Ceram Int* 48:32409–32417. <https://doi.org/10.1016/j.ceramint.2022.07.184>
23. Rajan HS, Kathirvel P (2021) Sustainable development of geopolymer binder using sodium silicate synthesized from agricultural waste. *J Clean Prod* 286:124959. <https://doi.org/10.1016/j.jclepro.2020.124959>
24. Tran-Nguyen PL, Ly K-P, Thanh LHV et al (2021) Facile synthesis of zeolite NaX using rice husk ash without pretreatment. *J Taiwan Inst Chem Eng* 123:338–345. <https://doi.org/10.1016/j.jtice.2021.05.009>
25. Tran YT, Lee J, Kumar P et al (2019) Natural zeolite and its application in concrete composite production. *Compos Part B Eng* 165:354–364. <https://doi.org/10.1016/j.compositesb.2018.12.084>
26. Narayanan S, Tamizhdurai P, Mangesh VL et al (2021) Recent advances in the synthesis and applications of mordenite zeolite – review. *RSC Adv* 11:250–267. <https://doi.org/10.1039/D0RA09434J>
27. Cao P, Li G, Jiang H et al (2021) Extraction and value-added utilization of alumina from coal fly ash via one-step hydrothermal process followed by carbonation. *J Clean Prod* 323:129174. <https://doi.org/10.1016/j.jclepro.2021.129174>
28. Nazir LSM, Yeong YF, Chew TL (2020) Methods and synthesis parameters affecting the formation of FAU type zeolite membrane and its separation performance: a review. *J Asian Ceram Soc* 8:553–571. <https://doi.org/10.1080/21870764.2020.1769816>
29. Wang J, Li M, Fu Y et al (2021) An ambient pressure method for synthesizing NaY zeolite. *Microporous Mesoporous Mater* 320:111073. <https://doi.org/10.1016/j.micromeso.2021.111073>
30. Kudinova AA, Poltoratckaya ME, Gabdulkhakov RR et al (2022) Parameters influence establishment of the petroleum coke genesis on the structure and properties of a highly porous carbon material obtained by activation of KOH. *J Porous Mater* 29:1599–1616. <https://doi.org/10.1007/s10934-022-01287-1>
31. Rozhkovskaya A, Rajapakse J, Millar GJ (2021) Synthesis of high-quality zeolite LTA from alum sludge generated in drinking water treatment plants. *J Environ Chem Eng* 9:104751. <https://doi.org/10.1016/j.jece.2020.104751>
32. Elboughdiri N (2020) The use of natural zeolite to remove heavy metals Cu (II), Pb (II) and Cd (II), from industrial wastewater. *Cogent Eng* 7. <https://doi.org/10.1080/23311916.2020.1782623>
33. Murukutti MK, Jena H (2022) Synthesis of nano-crystalline zeolite-A and zeolite-X from Indian coal fly ash, its characterization and performance evaluation for the removal of Cs⁺ and Sr²⁺ from simulated nuclear waste. *J Hazard Mater* 423:127085. <https://doi.org/10.1016/j.jhazmat.2021.127085>
34. Koohsaryan E, Anbia M, Maghsoodlu M (2020) Application of zeolites as non-phosphate detergent builders: a review. *J Environ Chem Eng* 8:104287. <https://doi.org/10.1016/j.jece.2020.104287>
35. Yusriadi Y, Ridayanti D, Sulastri E, Aanisah N (2022) The effect of tablet detergent wastewater using zeolite from rice husk ash on the chemical water quality and the growth of water hyacinth. *Tenside Surfactants Deterg* 59:433–440. <https://doi.org/10.1515/tsd-2022-2424>
36. Mordor Intelligence (2024) Sodium Silicate Market Size & Share Analysis - Growth Trends & Forecasts (2024 - 2029). <https://www.mordorintelligence.com/industry-reports/sodium-silicate-market>. Accessed 23.05.2024
37. Mordor Intelligence (2024) Zeolite Market Size & Share Analysis - Growth Trends & Forecasts (2024 - 2029). <https://www.mordorintelligence.com/industry-reports/zeolites-market>. Accessed 23.05.2024
38. Pyagay IN, Sizyakov VM, Svakhina YA et al (2023) Study of the process of obtaining water glass from silica gel for use in metallurgy. *iPolytech J* 27:598–610. <https://doi.org/10.21285/1814-3520-2023-3-598-610>
39. Mirfendereski M, Mohammadi T (2016) Effects of synthesis parameters on the characteristics of naa type zeolite nanoparticles. *World Congr Recent Adv Nanotechnol* 1–8. <https://doi.org/10.11159/icnnf.c16.113>
40. Aminullah RE, Yuliarto B, Irzaman (2018) Reduction of silicon dioxide from bamboo leaves and its analysis using energy dispersive x-ray and fourier transform-infrared. *IOP Conf Ser Earth Environ Sci* 209:012048. <https://doi.org/10.1088/1755-1315/209/1/012048>
41. Lee Y, DuMont JW, George SM (2015) Atomic layer etching of AlF₃ using sequential, self-limiting thermal reactions with Sn(acac)₂ and hydrogen fluoride. *J Phys Chem C* 119:25385–25393. <https://doi.org/10.1021/acs.jpcc.5b07236>
42. Merkulova M, Boudon V, Manceron L (2023) Analysis of high-resolution spectra of SiF₄ combination bands. *J Mol Spectrosc* 391:111738. <https://doi.org/10.1016/j.jms.2023.111738>
43. Kononov P, Kononova I, Moshnikov V et al (2022) Step-by-step modeling and demetallation experimental study on the porous structure in zeolites. *Molecules* 27:8156. <https://doi.org/10.3390/molecules27238156>
44. Collins F, Rozhkovskaya A, Outram JG, Millar GJ (2020) A critical review of waste resources, synthesis, and applications for Zeolite LTA. *Microporous Mesoporous Mater* 291:109667. <https://doi.org/10.1016/j.micromeso.2019.109667>
45. Dali Youcef L, López-Galindo A, Verdugo-Escamilla C, Belaroui LS (2020) Synthesis and characterization of zeolite LTA by hydrothermal transformation of a natural Algerian palygorskite. *Appl Clay Sci* 193:105690. <https://doi.org/10.1016/j.clay.2020.105690>
46. Rozhkovskaya A, Rajapakse J, Millar GJ (2021) Process engineering approach to conversion of alum sludge and waste glass into zeolite LTA for water softening. *J Water Process Eng* 43:102177. <https://doi.org/10.1016/j.jwpe.2021.102177>
47. Osacky M, Palkova H, Hudec P et al (2020) Effect of alkaline synthesis conditions on mineralogy, chemistry and surface properties of phillipsite, P and X zeolitic materials prepared from fine powdered perlite by-product. *Microporous Mesoporous Mater* 294:109852. <https://doi.org/10.1016/j.micromeso.2019.109852>
48. Al-Jubouri SM, Sabbar HA, Laft HA, Waisi BI (2019) Effect of synthesis parameters on the formation 4A zeolite crystals: characterization analysis and heavy metals uptake performance study for water treatment. *Desalin Water Treat* 165:290–300. <https://doi.org/10.5004/dwt.2019.24566>
49. Kong X, Qiu H, Zhang Y et al (2021) Seeded synthesis of all-silica CHA zeolites in diluted mother liquor. *Microporous Mesoporous Mater* 316:110914. <https://doi.org/10.1016/j.micromeso.2021.110914>
50. Ueno K, Yamada S, Negishi H et al (2020) Fabrication of pure-silica *BEA-type zeolite membranes on tubular silica supports coated with dilute synthesis gel via steam-assisted conversion. *Sep Purif Technol* 247:116934. <https://doi.org/10.1016/j.seppur.2020.116934>
51. Ayele L, Pérez-Pariente J, Chebude Y, Diaz I (2016) Synthesis of zeolite A using kaolin from Ethiopia and its application in detergents. *New J Chem* 40:3440–3446. <https://doi.org/10.1039/C5NJ03097H>
52. Xue Z, Li Z, Ma J et al (2014) Effective removal of Mg²⁺ and Ca²⁺ ions by mesoporous LTA zeolite. *Desalination* 341:10–18. <https://doi.org/10.1016/j.desal.2014.02.025>

Publisher's Note Springer Nature remains neutral with regard to jurisdictional claims in published maps and institutional affiliations.

Springer Nature or its licensor (e.g. a society or other partner) holds exclusive rights to this article under a publishing agreement with the author(s) or other rightsholder(s); author self-archiving of the accepted manuscript version of this article is solely governed by the terms of such publishing agreement and applicable law.